Pazur, J. H., Cepure, A., & Kane, J. A. (1973) *J. Biol. Chem. 248*, 270–284.
Sarkar, M., Liao, J., Kabat, E. A., Tanabe, T., & Ashwell, G. (1979) *J. Biol. Chem. 254*, 3170–3174.
Seglen, P. O. (1976) *Methods Cell Biol. 13*, 29–83.
Weigel, P. H. (1980) *J. Biol. Chem. 255*, 6111–6120.
Weigel, P. H., Naoi, M., Roseman, S., & Lee, Y. C. (1979) *Carbohydr. Res. 70*, 83–91.

Distance Measurements in Spin-Labeled Lysozyme†

Paul G. Schmidt* and Irwin D. Kuntz

ABSTRACT: The single His-15 of hen egg lysozyme reacts with 2,2,6,6-tetramethyl-4-(bromoacetamido)piperidinyl-1-oxy or 2,2,5,5-tetramethyl-3-(bromoacetamido)pyrrolidinyl-1-oxy to give a spin-labeled enzyme [Wien, R. W., Morrisett, J. D., & McConnell, H. M. (1972) *Biochemistry 11*, 3707–3716]. High-field ^1H NMR spectra (300 and 500 MHz) of these species in ^2H_2O contain protein peaks selectively broadened by dipolar coupling to the unpaired electron spin. While usually difficult to discern in the spectrum itself, broadened resonances are revealed in difference spectra obtained by subtracting the original spectrum from one taken after reduction of the nitroxide radical with ascorbate. The heights of difference spectra peaks are related in a simple way to r^{-6}, where r is the label to proton distance. These distances were used to solve for the location of the electron spin by using algorithms from distance geometry. The spin was found to lie in a hydrophobic groove between Phe-3 and Asp-87. These results demonstrate the feasibility of spin-labeling for accurate distance measurements in proteins through the use of distance geometry.

The time-averaged structure of any molecule can be determined if one measures a sufficient number of interatomic distances. Distance geometry (Crippen, 1981; Havel et al., 1979; Kuntz et al., 1979) provides the mathematical framework to convert distance measurements, with the associated experimental errors, into actual three-dimensional structures. A great many distances are needed to solve a structure. One estimate (Havel et al., 1979) suggests an order of 1000–2000 measurements would be required. This is in agreement with low-resolution X-ray diffraction studies on small proteins. In analogy with the diffraction methods the more measurements, the higher the resolution of the final result. NMR methods have considerable potential for such measurements, especially with the new two-dimensional techniques using the nuclear Overhauser effect (NOE). Methods such as NOESY (Jeener et al., 1979; Kumar et al., 1981), coupled with the high fields now available, provide semiquantitative estimates for a large number of interproton distances in proteins (Wüthrich et al., 1982). But even if all possible NOE's were determined to better than ±1-Å accuracy, the structure of a small protein would be underdetermined and could not be solved without the use of idealized models. The major difficulty is that the distances measured with NOE techniques are all short (less than 4 Å in proteins) compared to the radius of the molecule. Longer distances are required to complete the structure (Havel et al., 1979).

Paramagnetic probes offer another avenue to intramolecular distances. Because of the great strength of the paramagnetic moment compared to the magnetic moment of the proton, line-broadening effects can be seen out to about 20 Å in molecules of ca. 10000 daltons (Wien et al., 1973; Krugh, 1976; Dwek et al., 1975). The two main types of probes are paramagnetic metal ions such as Mn^{2+} or Gd^{3+} and free radicals. Metal ions have been quite useful in special cases where well-defined binding sites exist (Campbell et al., 1975; Lee & Sykes, 1983). Nitroxide spin-labels appear to be more generally useful and offer the opportunity to put probes, one at a time, in several specific locations throughout a protein by taking advantage of the great variety of reactive groups available (Berliner, 1976; Likhtenshtein, 1976). The possibility of measuring many hundreds of 10–20-Å distances is well worth investigating.

As an initial test of this strategy, we have prepared a spin-labeled lysozyme derivative. Wien et al. (1972) showed that hen egg white lysozyme, labeled at His-15 with 2,2,5,5-tetramethyl-3-(bromoacetamido)pyrrolidinyl-1-oxy, induced broadening of proton resonances from inhibitors binding more than 15 Å away. They checked to see if resonances from the protein could be likewise measured, but the spin-labeled lysozyme spectrum was devoid of resolution. Addition of ascorbate reduced the nitroxide to the diamagnetic hydroxylamine, after which the NMR spectrum sharpened up.

The early work of Wien et al. (1972) was limited by the low magnetic field employed (23 kG, 100-MHz ^1H). Without spectral resolution of the labeled protein, changes in line widths due to dipolar broadening from the free electron could not be determined. We have now measured spin-labeled lysozyme at 300 and 500 MHz. Increased dispersion at these high fields provides much better resolution in spectra of the paramagnetic enzyme. Equally important was our ability to work at much lower protein concentration because of greatly increased sensitivity. High concentrations lead to substantial broadening even at 300 MHz due to intermolecular effects. Finally, we used difference spectroscopy to quantitate line-broadening effects (Campbell et al., 1975). We subtracted a spectrum of paramagnetic spin-labeled protein from a spectrum taken after reduction of the label to the diamagnetic hydroxylamine. This procedure results in a greatly simplified trace containing

† From the Oklahoma Medical Research Foundation, University of Oklahoma Health Sciences Center, Oklahoma City, Oklahoma 73104 (P.G.S.), and the Department of Pharmaceutical Chemistry, University of California, San Francisco, San Francisco, California 94143 (I.D.K.).
Received January 16, 1984. Financially supported by National Institutes of Health Grants GM 19267 and GM 31497 to I.D.K. and Grant GM 25703 to P.G.S. and Research Career Development Award AM00525 to P.G.S.
* Address correspondence to this author at Vestar Research Inc., Pasadena, CA 91106.

0006-2960/84/0423-4261$01.50/0

Table I: Amino Acid Analysis of Spin-Labeled Lysozyme: Reaction of II + Lysozyme

AA	peak 1[a]	peak 2[a]	lysozyme[e]	theor
Asp	20.8	21.0	21.1	21
Thr	6.5	6.7	6.8	7
Ser	9.6	9.2	9.4	10
Glu	5.0	4.9	5.4	5
Pro	2.3	2.3	4.2	2
Gly	11.7	11.9	11.8	12
Ala	12.1	12.2	12.1	12
Cys[c]				8
Val[b]	5.2	5.4	5.5	6
Met	2.0	1.9	2.1	2
Ile[b]	4.7	5.1	4.2	7
Leu	7.1	7.4	6.9	7
Tyr	2.7	2.8	2.9	3
Phe	2.8	2.9	3.0	3
His	*d*	0.7	1.1	1
Lys	5.6	5.6	6.0	6
Arg	11.0	10.8	10.9	11

[a] HPLC first major peak (1) and second major peak (2). [b] Low values due to incomplete hydrolysis. [c] Not accurately determined under conditions used. [d] Not detected. [e] Commercial enzyme.

only peaks from residues near the label since difference spectral amplitudes are related to the inverse sixth power of label–proton distance.

Proton–electron distances for spin-labeled lysozyme were used in the distance geometry program, along with atomic coordinates from the lysozyme crystal structure, to solve for the position of the nitroxide radical. The program returned a well-defined location for the label near the surface of lysozyme. This result suggests that spin-labels provide a useful way to measure distances in proteins, and it points the way to determining protein structures in solution by distance geometry.

Materials and Methods

Hen egg white lysozyme (salt free) was obtained from Worthington Biochemicals. 2,2,6,6-Tetramethyl-4-(bromoacetamido)piperidinyl-1-oxy (I) and 2,2,5,5-tetramethyl-3-(bromoacetamido)pyrrolidinyl-1-oxy (II) were from Aldrich. ^2H_2O (99.96 atom %; low paramagnetic ions) was from Aldrich. Other chemicals were reagent grade.

Spin-labeled lysozyme was prepared by the method of Wien et al. (1972). A total of 70 mg of protein was dissolved in 1 mL of 0.1 M sodium acetate, pH 5.5, and the pH restored with 1 M HCl. Then 13.9 mg of I or II was dissolved in 50 μL of MeOH and added to the protein solution. The mixture was stirred gently at 40 °C for 30–36 h, during which time the cloudy solution cleared up. The reaction mixture was desalted, and excess spin-label was removed by chromatography at room temperature on Sephadex G-25 using 0.1 M ammonium acetate to elute. Pooled protein fractions were lyophilized.

Desalted spin-labeled lysozyme was further purified by preparative high-performance liquid chromatography (HPLC) on carboxymethylated silica with 0.01 M sodium phosphate, pH 6.0, and a gradient of 0–0.5 M NaCl. The main peak, containing spin-labeled protein, eluted first, followed by a peak with unlabeled protein. Main peak fractions were pooled, dialyzed against water, and lyophilized.

Amino acid analysis of the major peak of II–lysozyme showed all residues present in the same number as authentic lysozyme except His which was at a level of <0.12 residue (Table I). The second peak on HPLC gave an analysis consistent with underivatized lysozyme.

NMR spectra were run at 300 MHz on a hybrid instrument using a CMS 70/50 magnet and probe (Cryomagnet Systems, Inc., Indianapolis, IN) and a Nicolet 1180 computer system.

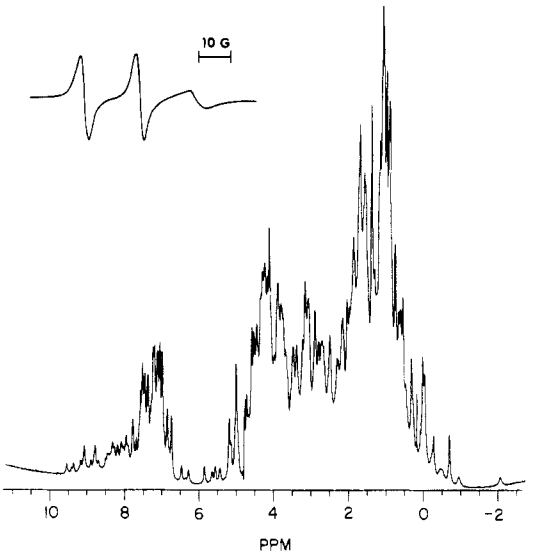

FIGURE 1: ^1H NMR spectrum of spin-labeled lysozyme: 2.5 mM I–lysozyme in D_2O, pH 5.3, 25 °C; 500-MHz 336 scans, 1-Hz broadening, solvent HDO presaturation; 1.5-s recycle time, 90° pulses. (Inset) ESR spectrum of I–lysozyme: 9.5 GHz; sample as above, 23 °C; 20-mW power, 2-G modulation, 0.3-s time constant, 8 min/100-G sweep; aqueous sample pH 5; glass capillary sample tube.

Spectra at 500 MHz were taken on a Nicolet instrument at the University of California, Davis. The solvent ^2H_2O peak was used for a field-frequency lock. The methyl resonance of Met-12 was used as an internal standard since its position is essentially invariant with pH and temperature (Poulsen et al., 1980).

Protein samples for NMR were dissolved in 0.4 mL of 0.1 M oxalate–D_2O buffer, pH* 5.2. The solution was lyophilized with readdition of 99.96 atom % ^2H_2O to a volume of 0.4 mL. Residual water was suppressed by presaturation. After a spectrum of spin-labeled protein was collected, 0.2 M sodium ascorbate in D_2O, adjusted to pH* 5.2, was added to a concentration of 5 mM to reduce the label. Following a 10–20-min period to allow complete reduction, another spectrum was recorded under the same conditions. The two spectra were subtracted in the computer with a correction for the 2.5% volume increase after addition of ascorbate.

Results and Discussion

An electron spin resonance (ESR) spectrum of lysozyme spin-labeled with I is shown in Figure 1 (insert). Since the outer extrema are separated by 39 G, the label is moderately immobilized relative to the enzyme. We observed similar spectra for lysozyme with label II as did Wien et al. (1972) for the same derivative.

A 500-MHz ^1H NMR spectrum of 2.5 mM spin-labeled I–lysozyme in D_2O is shown in Figure 1. It is very similar to spectra of unlabeled lysozyme taken under the same conditions. On the other hand, spectra of spin-labeled lysozyme above 5 mM concentration showed substantial general peak broadening, which increased with increasing concentration. We speculate that Wien et al. (1972) had to use such a high concentration at 100 MHz to observe the protein spectrum that intermolecular effects wiped out any resolution. Two effects are at work at high concentrations of labeled protein. First, general paramagnetic broadening is a factor. Second, self-association of lysozyme will increase with concentration. Even without the spin-label, this would lead to broader peaks because of increased rotational correlation times. Further, specific intermolecular relaxation effects will occur if the label is near amino acids on the partner protein in a self-association

complex. This behavior may be present for a few resonances in spin-labeled lysozyme (vide infra). In any case, concentration-dependent effects can certainly be important.

Does the spin-label perturb the protein structure? This is an important question since, in general, one is interested in the structure of the unmodified macromolecule. Chemical shifts of assigned peaks in the spin-labeled lysozyme spectrum are all very close to their positions in the unlabeled protein under similar conditions (Poulsen et al., 1980; Redfield et al., 1982; Delepierre et al., 1982). For example, the Met-105 methyl is within 0.01 ppm of its normal position at 0.0 ppm. Even groups that lie within 10 Å of the label have chemical shifts in accord with their normal values; viz., Phe-3, with 7.026, 7.219, and 7.511 ppm in lysozyme (Redfield et al., 1982) and 7.01, 7.22, and 7.50 ppm in II–lysozyme, is one of the closest side chains to the label. Not all peaks from label-side residues have been assigned, so the final word on label perturbation is not in. But it appears that the effects are not large and do not extend far into the protein.

When ascorbate was added to the spin-labeled protein solution, some sharpening of resonances was noted and new peaks appeared. Difference spectra show these changes most effectively. Figure 2 presents the difference spectrum for II–lysozyme at 35 °C, reduced with 5 mM ascorbate. Peaks at 3.74, 4.03, and 4.53 ppm belong to the added ascorbate. Prominent peaks near 1.35 ppm arise largely from methyl protons of the spin-label itself. Other peaks from the spin-label itself have not yet been assigned. The rest of the difference spectrum consists of protein resonances that had been more or less broadened by the free radical.

In Figure 2 the difference spectrum at 35 °C is compared with part of the ascorbate-reduced spectrum plotted at the same vertical gain. Note in the aromatic region that only a few peaks are left in the difference spectrum. Three prominent ones are at 7.50, 7.22, and 7.01 ppm; they correspond almost exactly with the assigned positions of Phe-3 (Redfield et al., 1982) and with the expected line shapes for CζH (triplet), Cϵ2H (triplet), and Cδ2H (doublet), respectively. A handful of slowly exchanging amide protons contribute to the difference spectrum in the region from 7.7 to 9 ppm. They are not firmly assigned at this time and were not used in the calculations below. In the aliphatic region Leu-17 $C\delta_2H_3$ has been assigned to the well-resolved peak at −0.68 ppm. It is easy to see that the difference spectrum peak has 0.25 times the intensity of the normal spectrum.

Difference spectra for aliphatic and aromatic regions at 45 °C are shown in parts A and B of Figure 3, respectively. By and large these traces are similar to the ones taken at 35 (Figure 2) and 23 °C (not shown). A notable exception is Ile-98 $C\gamma H_3$ at −0.26 ppm. Its relative amplitude in the difference spectrum decreases significantly at the higher temperature. An explanation is provided below.

Fractional amplitudes were measured (with the precision dependent on the signal/noise ratio and how well resolved they were) for assigned peaks that could be located reasonably unambiguously in difference spectra at 23, 35, and 45 °C. These peaks, their chemical shifts, and their fractional amplitudes (ΔAmp) are listed in Table II. In cases where peaks of interest in the normal spectrum (not base line corrected) overlapped severely with neighbors, their amplitudes and line widths were estimated on the basis of similar resolved resonances. We also estimated line widths directly using a convolution difference method (Campbell et al., 1973). Using both approaches, we estimate that uncertainties of up to ±0.2 in ΔAmp and ±25% in line width could arise in the worst case,

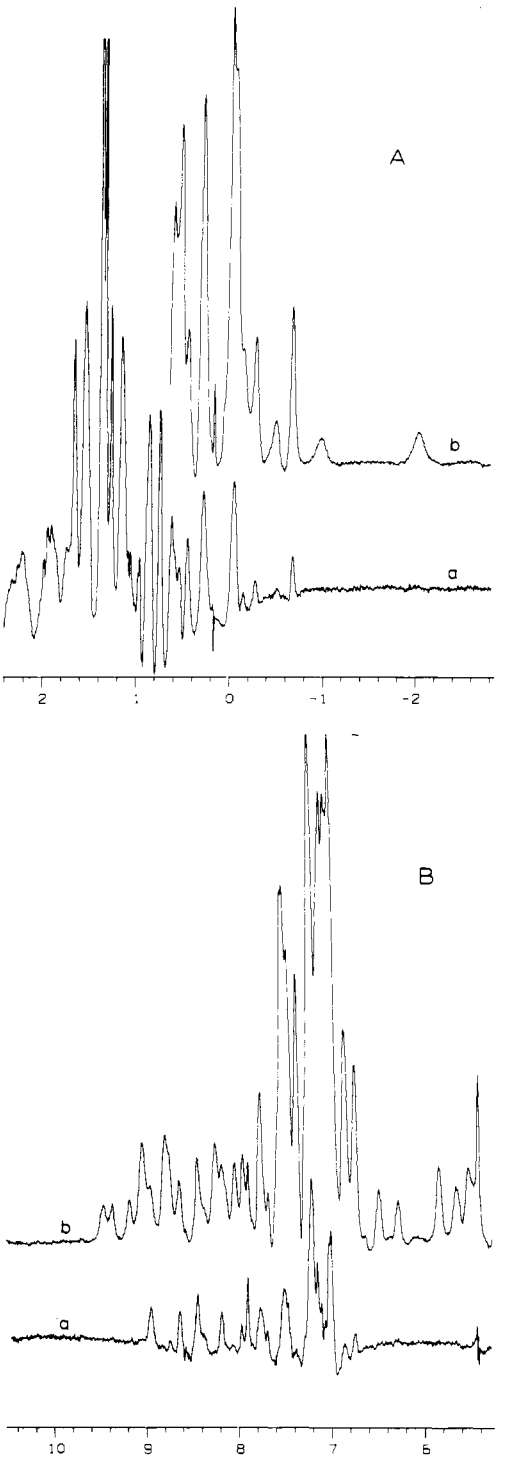

FIGURE 2: Difference spectrum of II–lysozyme minus II–lysozyme reduced (diamagnetic): 1.5 mM II–lysozyme in 0.1 M oxalate–D_2O, pH* 5.2, 35 °C; 300-MHz spectra, two blocks of 400 scans each, 2.4-s repetition delay, 90° pulses of 5.8 μs; 1-Hz broadening on the free induction decay, zero-filled to 8192 frequency domain points. (A) (a) Aliphatic region difference spectrum for oxidized minus reduced sample; (b) reduced sample spectrum at same gain as (a) (base line straightened). (B) Aromatic region. (a) and (b) as above.

but because of the r^{-6} dependence, errors in distance are minimized and lie within the overall limits given in Table II. In several cases a peak was confirmed to be absent from the difference spectrum, but we have not made use of this information at present.

Data Analysis

The relative intensity of a peak in the difference spectrum is related to how much broadening is induced by the label and

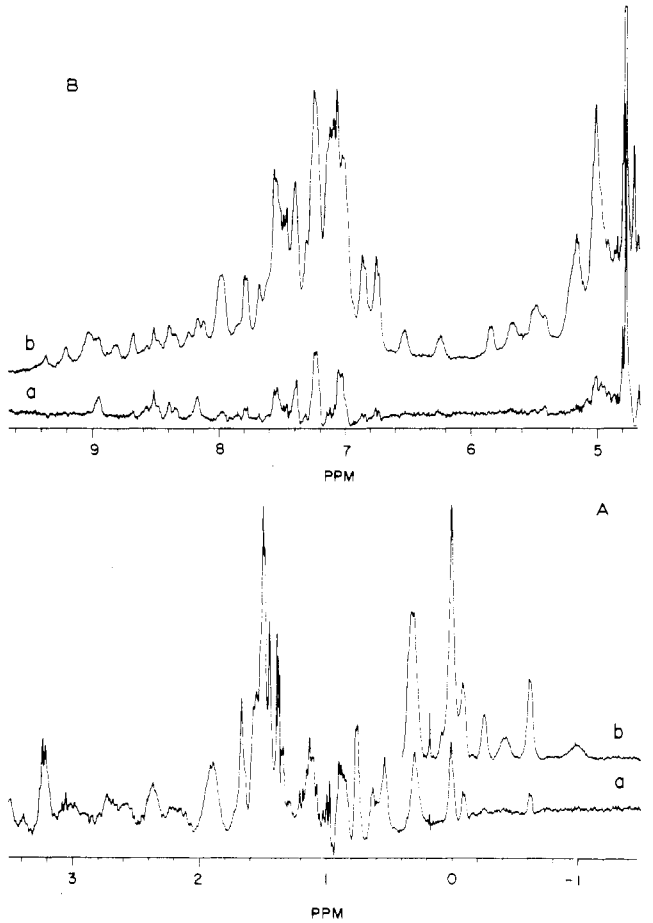

FIGURE 3: II–lysozyme difference spectrum: pH* 3.8; 45 °C. Other conditions and notations are as in Figure 2.

to the natural line width in the absence of a free radical. For singlets the expression for the fractional amplitude at the center of a difference spectrum peak is

$$\Delta\text{Amp} = 1 - W_A/W_B \quad (1)$$

where W_A is the line width of a peak in the diamagnetic protein and W_B is the total line width when the label is paramagnetic. $W_B = W_A + W_P$, where W_P is the paramagnetic contribution. In cases of multiplets, similar functions that also depend on coupling constant values were calculated from the classic NMR absorption line-shape equation.

Proton NMR line widths due to relaxation by the free radical are given by

$$W_P = Cr^{-6}\tau_R \quad (2)$$

where C is a constant containing the dipolar interaction, r is the electron spin–proton distance, and τ_R is the rotational correlation time for the label–proton vector. Since the spin-label is at least partly immobilized relative to the protein, τ_R is taken as the overall rotational correlation time for lysozyme (Wien et al., 1972), which, under the conditions of our experiment, is (0.5–1) × 10^{-8} s (Yguerabide, 1972; Dill & Allerhand, 1979; Bauer et al., 1975).

We used eq 1 and 2 to deduce the distance of the spin-label to the proton resonances of Table II with error limits established by considering (1) uncertainties in the experimental amplitudes, (2) uncertainties in the protein rotational correlation time, and (3) uncertainties resulting from solving for positions of the carbon atoms rather than those of the attached and mobile hydrogen atoms. Generally, the errors were ±3 Å except for larger estimates for quite short (≤10 Å) and long distances (>20 Å). In a few cases, errors were increased

Table II: Distances from NMR Spectra and Calculated Results from Distance Geometry Solution

residue	atom(s)	mult, J	23 °C				35 °C				45 °C					
			δ	LW	ΔAmp	distance	δ	LW	ΔAmp	distance	δ	LW	ΔAmp	distance	distance[a]	model[b]
Phe-3	CδH$_2$	d, 8.5	6.99	12	0.9	10	7.02	10	0.8	11	7.04	9	0.65	13	10 ± 3	11.0, 11.5
	CϵH$_2$	t, 8.5	7.21	12	0.9	10	7.22	12	0.9	10	7.23	8	0.86	11	10 ± 3	10.2, 9.7
	CζH	t, 8.5	7.5	12	0.9	10	7.52	12	0.9	10	7.55	7	0.7	13	10 ± 3	9.3
Met-12	CϵH$_3$	s	1.66	8	0.6	16	1.66	8	0.7	15	1.67	5	0.7	15	16 ± 3	16.6
His-15	CϵH	s	7.96	8	0.9	11	7.96	9	0.9	11		shifted			11 ± 3	8.8
Leu-17	Cδ1H$_3$	d, 7.0	−0.13	11	0.3	16	−0.13	10	0.1	21	−0.10	8	0.32	17	19 ± 3	16.2
	Cδ2H$_3$	d, 7.0	−0.73	11	0.35	16	−0.68	10	0.25	17	−0.63	8	0.22	17	17 ± 3	17.9
Tyr-23	CϵH$_2$	d, 8.5	6.74	8	0.2	17	6.74	10	0.15	20	6.75	7	0.11	21	22 ± 8	26.6, 25.7
Trp-28	CζH	t, 8.5	6.26	8	0.15	21	6.28	10	0.1	23	6.24	7	0.13	22	22 ± 3	20.9
Asn-39	CαH	m	5.47	(8)[c]	0.25	18		overlap			5.42	(5)	0.3	19	18 ± 3	15.3
Tyr-53	CδH$_2$	d, 8.5	7.14	8	0.25	17		overlap			7.14	6	0.08	21	22 ± 8	17.6
	CϵH$_2$	d, 8.5	6.85	8	0.15	19	6.85	10	0.15	19	6.85	7	0.07	22	22 ± 8	19.0
Asn-59	CαH	m	5.65	(8)	0.1	19		overlap			5.69	(5)	0.08	23	20 ± 3	22.1
Cys-64	CαH	m	5.84	8	0.1	20		overlap			5.85	(5)	0.04	27	25 ± 8	19.4
Asn-65	CαH	m	5.55	(8)	0.15	20		overlap			5.52	(5)	0.13	21	20 ± 2	20.8
Ile-88	CδH$_3$	t, 7.5	0.27	11	0.9	10	0.28	10	0.8	13	0.29	6	0.9	11	10 ± 4	10.7
	CγH$_3$	d, 7.0	0.75	8	0.9	10	0.75	6	0.9	10	0.75	7	0.9	10	10 ± 4	9.3
Val-92	Cγ1H$_3$	d, 6.0	0.44	8	0.6	14	0.45	10	0.6	13	0.51	7	0.6	13	12 ± 4	13.6
	Cγ2H$_3$	d, 6.0	0.61	8	0.8	11	0.62	10	0.6	13	0.64	7	0.7	12	12 ± 4	12.6
Ile-98	Cγ2H$_3$	d, 7.0	−0.32	8	0.3	16	−0.27	10	0.15	19	−0.26	8	0.08	21	20 ± 5	21.2
Trp-108	CζH	t, 7.5	6.48	8	0.1	23	6.48	10	0.05	24	6.54	6	0.05	26	25 ± 5	25.3

[a] Average calculated distance for protons to electron spin ± estimated error. [b] Spin to carbon atom distance from computed best-fit structure. Two values represent distances to individual atoms of a spin system. [c] Values in parentheses are estimated.

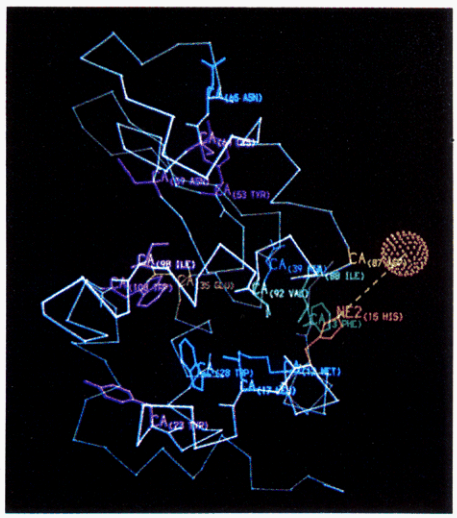

FIGURE 4: Location of spin-label electron spin in II–lysozyme. The size of the "ball" shows the approximate uncertainty in location of the label. The protein backbone is shown in white, His-15 is shown in orange, and assigned residues are shown with side chains in various colors depending on the distance from the label.

further for distances that appeared to be quite temperature dependent (Tyr-23 Cϵ, Tyr-53 Cϵ, Cys-64 Cα, Ile-98 Cγ, Trp-108 Cζ).

We used this information to ask a simple question: Are the data consistent with a single probe position given the known crystal structure for lysozyme? To explore this point, we took the atomic coordinates for triclinic lysozyme from the experiments of Phillips (Diamond, 1974) supplied by the Protein Data Bank, Brookhaven National Laboratories (see Figure 4). Optimization of the usual distance geometry error function as the probe position was varied let us examine how precisely the spin-label could be located, consistent with the assumption of a rigid, isotropically tumbling protein with a correlation time of approximately 10 ns. The probe was always found in a shallow groove in the protein surface, bounded by residues Phe-3, His-15, Asp-87, and Ile-88 on the side of the protein away from the active site cleft. The optimization procedure found a global minimum with zero residual error within a region of space given by the coordinates $x = 5 \pm 1$ Å, $y = 4 \pm 1$ Å, and $z = 14 \pm 1$ Å for all three temperatures. Variation of the error limits and the starting point for optimization showed that this solution is reasonably robust. The calculated distances for each resonance with the probe positioned at this location are given in Table II.

The most discordant aspect of the data is the large temperature dependence for certain distances. There are several possible sources for this effect. We presently feel that it arises from self-association of lysozyme at low temperature for the following reasons:

(1) This much temperature dependence for the rotational correlation time of the entire protein would require an unacceptable activation barrier (>15 kcal/mol) and would be expected to affect all proton to probe distances more or less equally given (eq 2).

(2) Increased reorientation of the probe would have the most effect on the shorter distances. Further, increased probe motion would cause some average distances to increase but others to decrease. We see only an increase in apparent distances and only (some of) the longer distances are involved.

(3) If part of the protein begins to move so that, on the average, the distance to the probe is increased, one would see temperature-dependent effects for the protons involved in the motion. We cannot rigorously dismiss such a mechanism but notice that, of the resonances involved, Tyr-53 is in the β sheet, Tyr-23 is on one loop, and Ile-98 and Trp-108 are on another loop. Concerted motion of these disparate regions of the molecule and, particularly, deformation of the β sheet by several angstroms seem unlikely.

(4) Self-association of lysozyme in solution is well-known for the native protein (Imoto et al., 1972), particularly at pH values above 5 due to Glu-35 ionization. A plausible self-association model can be established on the basis of the protein–protein interactions seen in the crystal. Specifically, Hogle et al. (1981) describe a dimer in which Glu-35 (in the active site) interacts with His-15, which holds the label. Residues relatively distant from His-15 in the monomeric species but close to Glu-35 will be selectively broadened in the dimer. Using the probe position, above, we find that all protons showing unusual temperature behavior are more than 15 Å from the label (in the monomer) and all are within 15 Å of Glu-35. While this observation does not form conclusive proof, it makes the self-association model the most consistent explanation of the unusual temperature effect.

Two more points can be made from the present analysis of the data. First, there is no need to invoke partial labeling (>10%) of non-histidine residues to explain any observations. Second, even a preliminary effort, such as this one, can play a role in the laborious task of assigning the proton spectrum. For instance, the lysine and/or arginine signals at 3.2 ppm in the 45 °C spectrum can only come from Lys-1 and/or Arg-14 if the spin-label position is correct.

Conclusion

The conclusions we draw from this initial set of experiments are as follows: (1) The distances derived from the spin-label results for lysozyme in solution are consistent with the atomic coordinates taken from the lysozyme crystal structure within an uncertainty of a few angstroms. (2) The data are explainable assuming an immobilized probe in a relatively well-defined location. (3) The apparent temperature dependence of some of the probe to proton distances is best explained as self-association of lysozyme into specific dimers. (4) The spin-label technique is potentially quite suitable for gathering intramolecular distances. It is a useful adjunct to NOE measurements in small proteins. In lysozyme, the approach is limited by lack of complete assignments and by the overlap of resonances. The first problem is being rapidly ameliorated by the work in Dobson's laboratory. The second problem requires careful attention.

Acknowledgments

We are grateful to our colleagues Drs. V. Basus, N. Oppenheimer, and T. James for many discussions. Dr. C. Dobson kindly provided results prior to publication. Cathy Yen provided excellent technical assistance. Figure 4 was made with the kind assistance of Robert Tilton at the UCSF Computer Graphics Laboratory, funded by Research Resources Grant 1081 to R. Langridge.

Registry No. I, 24567-97-3; II, 17932-40-0; lysozyme, 9001-63-2.

References

Bauer, D. R., Opella, S. J., Nelson, D. J., & Pecora, R. (1975) *J. Am. Chem. Soc. 97*, 2580–2582.

Berliner, L. J. (1976) *Spin Labeling Theory and Applications*, Academic Press, New York.

Campbell, I. D., Dobson, C. M., Williams, R. J. P., & Xavier, A. V. (1973) *J. Magn. Reson. 11*, 172–181.

Campbell, I. D., Dobson, C. M., & Williams, R. J. P. (1975) *Proc. R. Soc. London, Ser. A 345*, 23–40.

Crippen, G. M. (1981) *Distance Geometry and Conformational Calculations*, Research Studies Press, Wiley, New York.

Delepierre, M., Dobson, C. M., & Poulsen, F. M. (1982) *Biochemistry 21*, 4756–4761.

Diamond, R. (1974) *J. Mol. Biol. 82*, 371–391.

Dill, K., & Allerhand, A. (1979) *J. Am. Chem. Soc. 101*, 4376–4378.

Dwek, R. A., Knott, J. C. A., March, D., McLaughlin, A. C., Press, E. M., Price, N. C., & White, A. I. (1975) *Eur. J. Biochem. 53*, 25–39.

Havel, T. F., Crippen, G. M., & Kuntz, I. D. (1979) *Biopolymers 18*, 73–81.

Hogle, J., Rao, S. T., Mallikarjunan, M., Beddell, C., McMullan, R. K., & Sundaralingam, M. (1981) *Acta Crystalliogr., Sect. B B37*, 591–597.

Imoto, T., Johnson, L. N., North, A. C. T., Phillips, D. C., & Rupley, J. A. (1972) *Enzymes, 3rd Ed. 7*, 665–868.

Jeener, J., Meier, B. H., Bachmann, P., & Ernst, R. R. (1979) *J. Chem. Phys. 71*, 4546–4553.

Krugh, T. R. (1976) in *Spin Labeling—Theory and Applications* (Berliner, L. J., Ed.) pp 339–372, Academic Press, New York.

Kumar, A., Wagner, G., Ernst, R. R., & Wüthrich, K. (1981) *J. Am. Chem. Soc. 103*, 3654–3658.

Kuntz, I. D., Crippen, G. M., & Kollman, P. A. (1979) *Biopolymers 18*, 939–957.

Lee, L., & Sykes, B. D. (1983) *Biochemistry 22*, 4366–4373.

Likhtenshtein, G. I. (1976) *Spin Labeling Methods in Molecular Biology*, Chapter 2, Wiley, New York.

Poulsen, F. M., Hoch, J. C., & Dobson, C. M. (1980) *Biochemistry 19*, 2597–2607.

Redfield, C., Poulsen, F. M., & Dobson, C. M. (1982) *Eur. J. Biochem. 128*, 527–531.

Wien, R. W., Morrisett, J. D., & McConnell, H. M. (1972) *Biochemistry 11*, 3707–3716.

Wüthrich, K., Wider, G., Wagner, G., & Braun, W. (1982) *J. Mol. Biol. 155*, 311–346.

Yguerabide, J. (1972) *Methods Enzymol. 26* (*C*), 528.